orthopaedics and dentistry, as it is a renowned antibacterial and bone repairing material that possesses high fracture resistance, ductility and weight to strength ratio. As titania does not support cell adhesion and growth well, functionalised and coated forms of titania can be used [12]. Additionally, titania has been applied on a wide range of application areas such as, antibacterial coatings [14], photocatalytic degradation of organic pollutants [15], self-cleaning surfaces [16], and water and air purifiers [17].
The present study has focused on the synthesis of TiO_2 NPs and their biological applications with special emphasis on antimicrobial activities. The prepared TiO_2 NPs were characterized by UV-Vis, FTIR, XRD, SEM and TEM.

2. Materials And Methods

2.1. Equipments

UV-Vis spectrophotometer (Varian, Carry 5000) was used to measure absorption with 1- cm path length quartz cuvettes, FTIR spectrophotometer (Thermo Nicolet, Avatar 370) was employed for embedded function group identification and Bruker AXS Advance powder X-ray diffractometer was used for characterization of crystalline nature of sample. Morphological analyses were carried out using Scanning Electron Microscopy(SEM) with a JEOL Model JSM - 6390LV instrument and Jeol/JEM 2100 High Resolution Transmission Electron Microscope.

2.2. Chemicals And Microbial Cultures

Titanium nitrate tetrahydrate $Ti(NO_3)4.4H_2O$, and urea were purchased from HiMedia. All the chemicals used in this work were of analytical grades. Milli-Q distilled water was used for nanoparticle synthesis. Gram positive bacteria (*Bacillus subtilis* MTCC 1305 and *Staphylococcus aureus* MTCC 3160) and gram negative bacteria (*Escherichia coli* MTCC 443 and *Pseudomonas aeruginosa* MTCC 2453) were procured from Microbial Type Culture Collection (MTCC) and used as test organisms. All the cultures were stored and maintained at 4^0C.

2.3. Synthesis Of Tio2 Nanoparticles

Synthesis of TiO_2 NPs was carried out as follows: 0.5 mmol of Titanium nitrate tetrahydrate $Ti(NO_3)4.4H_2O$ and a trivial quantity of urea $(CO(NH_2)2)$ were dissolved in 70 ml of deionized water and the mixture was continuously stirred. Then, the homogenous solution was transferred into a 100ml conical flask, teflon lined and autoclaved for 12 h at 180 °C. Once the process was completed, the solution was then shifted to room temperature and allowed to cool. Finally, a white precipitate was formed. The precipitate was washed numerous times with plenty of distilled water and absolute ethanol and subsequently dried overnight at 353 K. Eventually, the white precipitate was dried in air at 450 °C for 15 hours [20].

2.4. Characterization Of Tio2 Nanoparticles

The morphology and the size of the TiO_2 NPs were characterized by Scanning Electron Microscopy (SEM). TiO_2 NPs size, morphology and distribution were examined by the High Resolution Transmission Electron Microscope. UV- vis spectrophotometer was used to measure the absorption spectra of the synthesized nanoparticles in the range of 300 nm and 800 nm. The readings were taken at intervals of 1 nm with the scan rate 600 nm/min. The as-prepared nanoparticles were subjected to functional group analysis using FTIR spectrophotometer. The samples were prepared using KBr pellet method in 1:99 ratios at room temperature. The samples were scanned in the spectral range of 4000-400 cm^{-1} with the resolution of 2 cm^{-1}. X-ray diffraction (XRD) patterns were collected using a powder X-ray diffractometer. The XRD pattern of synthesized sample was obtained inside the special XRD cell designed to avoid the reaction of air sensitive samples with atmospheric oxygen [21].

2.5. Antibacterial Assay Of Tio2 Nanoparticles

The antimicrobial activity of the TiO_2 NPs was evaluated with well disc diffusion method. The experiment was conducted against reference gram positive (*B. subtilis* and *S.aureus*) and gram negative bacteria (*E. coli* and *P. aeruginosa*) procured from Microbial Type Culture Collection (MTCC), Chandigarh, India. An inoculum size of 10^5 cells/ml was used to spread on the Mueller-Hinton Agar (MHA, HiMedia, India). In Brief, 20 ml of MHA was poured into petri dishes and allowed to solidify. Then, 6 mm thick sterile discs were placed appropriately on petridishes. Finally, different concentrations of TiO_2 Nps (20, 40, 80 and 100 µg/ml) were loaded on each disc and 50% ethanol was used as a negative control. All the plates were incubated at 37 °C for 24 hours and the respective inhibition zones were measured. Each test was performed in triplicates under the same set of conditions for reproducibility [22].

3. Results And Discussion

3.1. UV-vis and FTIR absorption spectra

Fig. 1 represents the UV-vis absorption spectrum of the synthesized TiO_2 NPs. In this study, the formation of milky white colloidal solution indicated the conversion of Titanium nitrate tetrahydrate $Ti(NO_3)4.4H_2O$ into nanosized TiO_2 colloidal particles. Further, their physical properties were examined using UV-Visible spectroscopy and FTIR techniques. The synthesis of nanosized TiO_2 colloidal particles was thus confirmed with the absorption spectra between 300 nm and 800 nm (Fig. 1). The UV-vis peaks denoted the direct recombination between electrons in the conduction band and holes in the valence band [23].

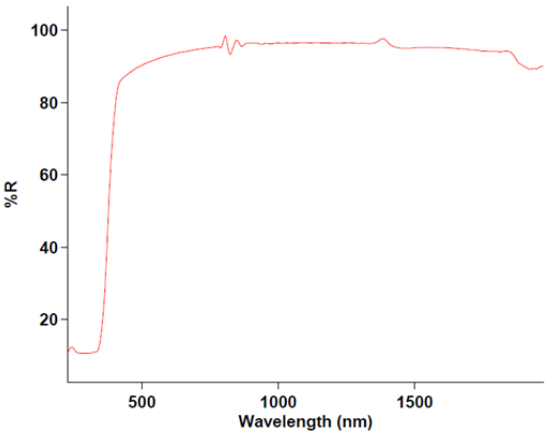

Fig.1 UV-vis absorption spectrum for the synthesized TiO_2 NPs

The functional groups of nanoparticles were established by FTIR spectrum. Fig. 2 represents the FTIR absorption spectrum of the synthesized nanoparticles. Spectrum of TiO_2 NPs had shown an intense peak at 3414.66 cm^{-1} due to OH stretching mode. Appearance of characteristic peak at 1626.54 cm^{-1} denoted the presence of crystallographic H_2O molecules i.e O-H bend. The broad peak at 499.36 cm^{-1} and 751.42 cm^{-1} represented Ti-O band and Ti–O–Ti skeletal frequency, respectively [24].

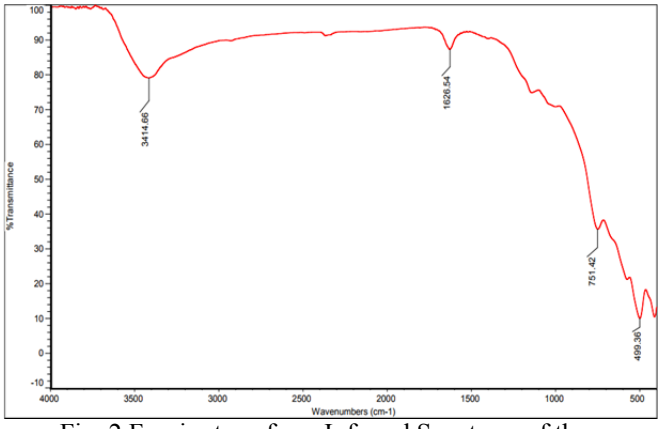

Fig. 2 Fourier transform Infrared Spectrum of the synthesized TiO_2 NPs

3.2. scanning electron microscopy and transmission electron microscopy

Fig. 3 depicts the SEM micrographs of TiO_2 NPs. SEM micrographs exposed cluster appearances with crystalline natures. However, spherical structures of size less than 20 nm with irregular surface morphologies denoted an increased grain size due to the increase in temperature leading to crystalline as well as grain growth. The stony appearance might have been due to the aggregation of TiO_2 NPs ranging between 145.6-205.91nm in size.

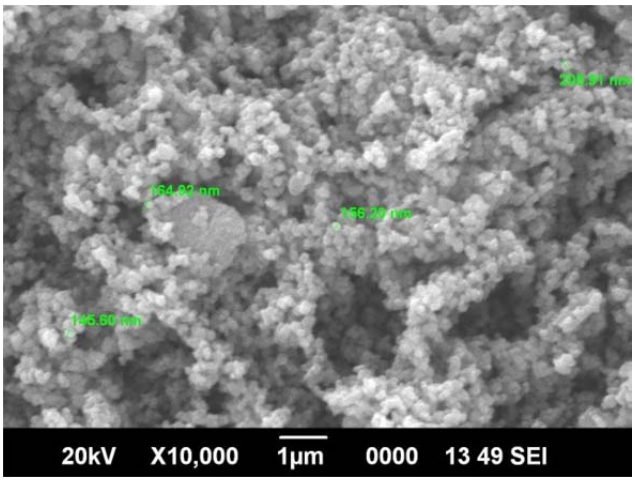

Fig. 3 Scanning Electron Micrographs of the synthesized TiO_2 NPs

Fig. 4 shows the TEM reflection and size allocation of TiO_2 NPs, which were a mixture of diverse sizes and shapes. The particles were almost spherical or irregular spherical with particle size ranging between 30.78nm - 51.56nm.

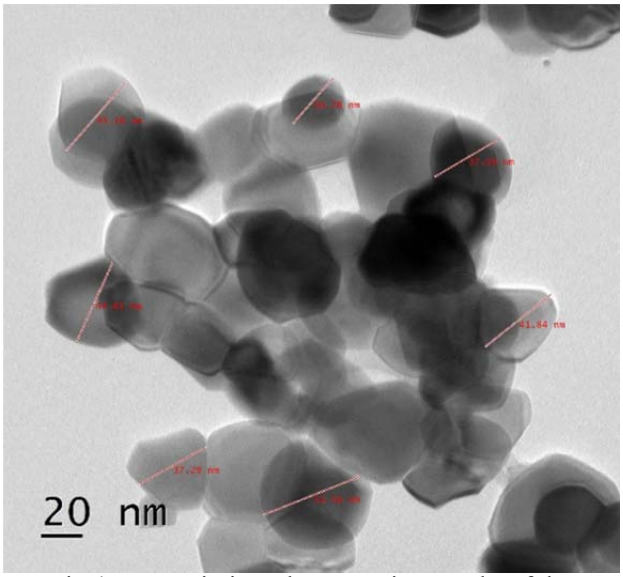

Fig 4. Transmission Electron Micrographs of the synthesized TiO_2 NPs

3.3 X-ray diffraction

XRD is of great importance in the microstructure characterization of complex, multiphase and single phase materials. The application of XRD enables not only qualitative and quantitative phase analysis but also microstructure characterization The significant peaks observed from 2 theta scale were at 25°, 37°, 47°, 54°, and 62° which corresponded to (1,0,1), (0,0,4), (2,0,0), (2,1,1) and (3,1,0). The peaks from the XRD pattern were identified from comparison with Joint Committee for Powder Diffraction studies (JCPDS) and the intense peak at 25.07 confirmed TiO_2 [26]. The average particle size was estimated using Debye-Scherer equation and inner planar spacing by Bragg's Law as shown in Eq. (1) and (2)

$$D = \frac{0.9\,\lambda}{\beta\, Cos\,\theta} \qquad (1)$$

$$\lambda = 2d\, Sin\theta \qquad (2)$$

Where, λ is the wavelength of X-ray (0.154 nm), β is an angular or line broadening at full width at half maximum (FWHM), θ is a diffraction angle, D is the particle diameter in nm and d represents planar spacing. The crystalline size of the synthesised nanoparticle was found to be in the range of 47 to 50 nm and inter planar spacing between atoms was in the range of 0.35 to 0.15 nm. The nanoparticle size analyzed from TEM images was found to be close to those calculated from Debye-Scherer equation.

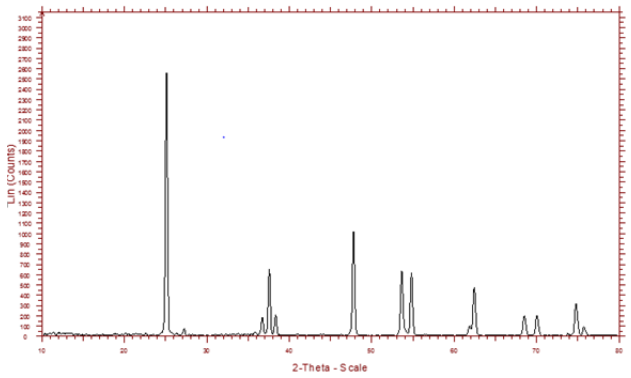

Fig. 5 X-ray Diffraction analysis of the synthesized TiO_2NPs

3.4. Antibacterial activity

Nanomaterials reveal strong inhibiting effects towards a broadened spectrum of bacterial strains. The metal oxides transmit a positive charge while the microorganisms hold a negative charge. Hence, electromagnetic attractions between microorganisms and metal oxides lead to oxidization and finally result in the death of microorganisms. Antimicrobial activity of nanoparticles was determined by disc diffusion method against *E. coli*, *P. aeruginosa*, *S. aureus* and *B. subtilis* as shown in Fig. 6. The results show that TiO_2 NPs had potential inhibitory action against *P. aeruginosa* and *S. aureus* while there was less action against *B. subtilis and E. coli*. It was also observed that the TiO_2 NPs have shown better inhibitory action even at lower concentrations (Fig.7). In the previous study conducted on ZrO_2 NPs involving their applications in dental care, MIC values against the most prevalent microorganisms were also obvious in the range of 40-80 µg/ml [27].

A better antibacterial activity against gram negative bacteria may be due to the negatively charged cell wall of bacteria being ruptured by positively charged titanium ions from titania nanoparticles causing discharge of proteinaceous and other intracellular components. It has also been proposed that decrease in intracellular ATP levels could lead to destabilization in the outer and plasma membranes. Several mechanisms were suggested to emphasize the antimicrobial activity of TiO_2NPs: bacterial cell wall structure of bacteria , thickness of the membrane cell wall, release of titanium ions from Titania, the generation of hydrogen peroxide which is cytotoxic, reactive oxygen species (ROS) from TiO_2 nanoparticles [5]. During photo-catalysis of TiO_2 nanoparticles, cells would get inactivated and metabolic chains get disrupted by the disability to transport ions. These factors have resulted in the biocidal activity of TiO_2 NPs. Thus, TiO_2 NPs proved to be a potential antibacterial agent against both grampositive and gram- negative microorganisms though revealed to be most effective against gram negative bacteria.

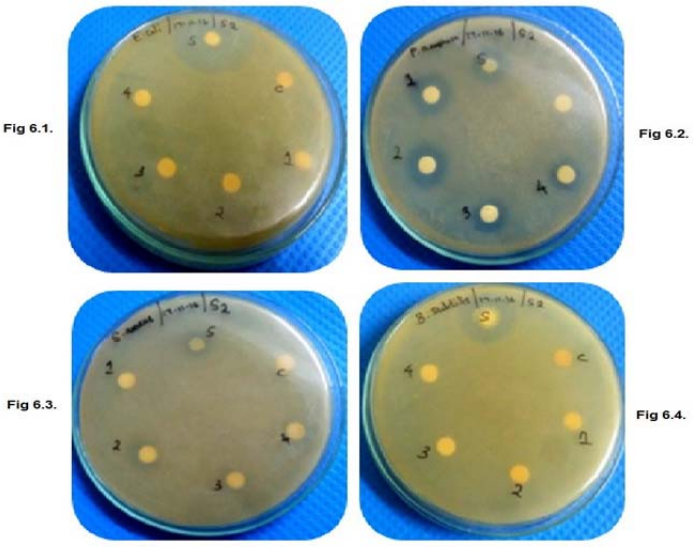

Fig 6.1, Antimicrobial (E. Coli) activity of the synthesized TiO_2 nanoparticles
Fig 6.2, Antimicrobial (P. Aeruginosa) activity of the synthesized TiO_2 nanoparticles
Fig 6.3, Antimicrobial (S. Aureus) activity of the synthesized TiO_2 nanoparticles
Fig 6.4, Antimicrobial (B. Sublitis) activity of the synthesized TiO_2 nanoparticles

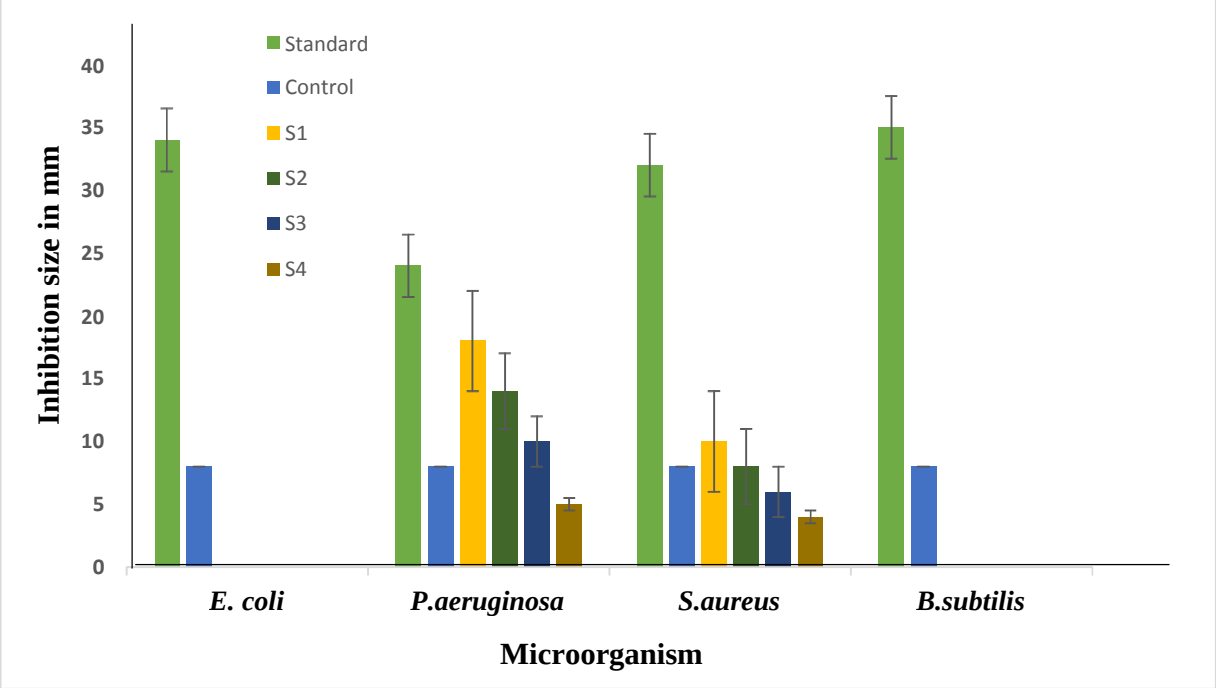

Fig 7. Antibacterial activity of the synthesized TiO_2 NPs

4. Conclusion

The present study has illustrated the synthesis of TiO2 NPs and their subsequent characterization has been done using UV-vis spectroscopy, FTIR, XRD, SEM and TEM. The UV-visible peaks indicated the formation of TiO2 NPs from Titanium nitrate tetra hydrate Ti(NO3)4.4H2O. Presence of crystallographic water molecule and the characteristic peaks of Ti-O stretching were also confirmed through FTIR. TiO2 NPs were of crystalline nature and spherical in shape that have been identified through XRD, SEM and TEM analysis. The antibacterial activity of TiO2 NPs was observed against both gram-positive and gram-negative bacteria and the results showed that TiO2 NPs had potential inhibitory actions against *P. aeruginosa* and *S. aureus* while there was less action against *B. subtilis and E. coli*. It was also observed that TiO2 NPs did show better inhibitory action even at lower concentration probably due to the positively charged TiO2 NPs against cell membrane. Thus, TiO2 NPs could be recommended for biomedical applications especially in dental and ortho-care as they are inert and less toxic.

References

[1] Boyer, C., Whittaker, M. R., Bulmus, V., Liu, J., & Davis, T. P., *NPG Asia Materials*. 2010, *2*(1), 23–30.

[2] Sanvicens, N., & Marco, M. P., *Trends in Biotechnology*. 2008, *26*(8), 425–433.

[3] Morigi, V., Tocchio, A., Bellavite Pellegrini, C., Sakamoto, J. H., Arnone, M., & Tasciotti, E., *Journal of Drug Delivery*, 2012(*2012*), 1–7.

[4] Laroui, H., Rakhya, P., Xiao, B., Viennois, E., & Merlin, D., *Digestive and Liver Disease*, 2013, *45*(*12*), 995–1002.

[5] Sundrarajan, M., Bama, K., Bhavani, M., Jegatheeswaran, S., Ambika, S., Sangili, A., … Sumathi, R., *Journal of Photochemistry and Photobiology B: Biology*, 2017, *171*(*April*), 117–124.

[6] Rehan, M., & Kale, G. M., *CrystEngComm*, 2011,*2011(May)* 3725–3732.

[7] Byranvand, M. M., Kharat, A. N., Fatholahi, L., & Beiranvand, Z. M. (2013). A Review on Synthesis of Nano-TiO 2 via Different Methods, *3*, 1–9.

[8] Imran, M., Riaz, S., & Naseem, S. *Materials Today, Elsevier Ltd.* (2012), *Proceedings* (Vol. 2).

[9] Yazdi, A. S., Guarda, G., Riteau, N., Drexler, S. K., Tardivel, A., Couillin, I., & Tschopp. J., *Proceedings of the National Academy of Sciences of the United States of America*, 2010, *107*(45), 19449–19454.

[10] Maness, P., Smolinski, S., Blake, D. M., Huang, Z., Wolfrum, E. J., & Jacoby, W. A., *Appl Environ Microbiol*, 1999, *65*(9), 4094–4098.

[11] Tsuang, Y.-H., Sun, J.-S., Huang, Y.-C., Lu, C.-H., Chang, W. H.-S., & Wang, C., *Artificial Organs*, 2008, *32*(2), 167–174.

[12] Khaled, S. M., Sui, R., Charpentier, P. A., & Rizkalla, A. S., *Langmuir*, 2007, *23*(7), 3988–3995.

[13] Su, W., Wang, S., Wang, X., Fu, X., & Weng, J., *Surface and Coatings Technology*, 2010, *205*(2), 465–469.

[14] Lin, H., Xu, Z., Wang, X., Long, J., Su, W., Fu, X., & Lin, Q., *Journal of Biomedical Materials Research - Part B Applied Biomaterials*, 2008, *87*(2), 425–431.

[15] Yew, S. P., Tang, H. Y., & Sudesh, K., *Polymer Degradation and Stability*, 2006, *91*(8), 1800–1807.

[16] Onar, N., Aksit, A. C., Sen, Y., & Mutlu, M., *Fibers and Polymers*, 2011, *12*(4), 461–470.

[17] Dastjerdi, R., & Montazer, M., *Colloids and Surfaces B: Biointerfaces*, 2010, *79*(1), 5–18.

[18] Renuka, N. K., & Nikhila, M. P., *Journal of Chemical and Pharmaceutical Sciences* 2016, *2016–Janua*(1), 85–90.

[19] Li, L., Ma, W., Cheng, X., Ren, X., Xie, Z., & Liang, J., *Colloids and Surfaces B: Biointerfaces*, 2016, *148*, 511–517.

[20] R. Shanmuganathan, D. MubarakAli, D. Prabakar, H. Muthukumar, N. Thajuddin, S.S. Kumar, A. Pugazhendhi., *Environmental Science and Pollution Research*, 2017, (*June*) 1-9.

[21] M. Davoodbasha, S.-Y. Lee, S.-C. Kim, J.-W. Kim., *RSC Adv*,.2015, *(5),* 35052-35060.

[22] V.S. Ramkumar, A. Pugazhendhi, K. Gopalakrishnan, P. Sivagurunathan, G.D. Saratale, T.N.B. Dung, E. Kannapiran., *Biotechnology Reports,* 2017, *14*, 1-7.

[23] Vijayalakshmi, R., & Rajendran, V., *Scholar Research Library*, 2012, *4*(2), 1183–1190.

[24] Renuka N. K.* and Nikhila M.P., *Journal of Chemical and Pharmaceutical Sciences* 2016, ISSN: 0974-2115

[25] Chauhan, V. P., & Jain, R. K., *Nature Publishing Group*, 2013, *12*(11), 958–962.

[26] Ba-Abbad M, Kadhum AH, Mohamad A, Takriff MS, Sopian K., *Int.J.Electrochem.Sci.* 2012, *7*, 4871-4888.

[27] Bani, J., Pugazhendhi, A., & Venis, R., *Microbial Pathogenesis*, 2017, *110*, 245–251.

[28] Albar, J. P., Barbas, C., Martins, V. A. P., Ferna, M., & Ferrer, M. (n.d.). Understanding the antimicrobial bacterium, 1–9.